

Josephson effect in double-barrier superconductor-ferromagnet junctions

Z. Radović,¹ N. Lazarides,² and N. Flytzanis³

¹*Department of Physics, University of Belgrade, P.O. Box 368, 11001 Belgrade, Yugoslavia*

²*Department of Materials Science and Technology,
University of Crete, P.O. Box 2208, 71003 Heraklion, Greece*

³*Department of Physics, University of Crete, P.O. Box 2208, 71003 Heraklion, Greece*

We study the Josephson effect in ballistic double-barrier SIFS planar junctions, consisting of bulk superconductors (S), a clean metallic ferromagnet (F), and insulating interfaces (I). We solve the scattering problem based on the Bogoliubov-de Gennes equations and derive a general expression for the dc Josephson current, valid for arbitrary interfacial transparency and Fermi wave vectors mismatch (FWVM). We consider the coherent regime in which quasiparticle transmission resonances contribute significantly to the Andreev process. The Josephson current is calculated for various parameters of the junction, and the influence of both interfacial transparency and FWVM is analyzed. For thin layers of strong ferromagnet and finite interfacial transparency, we find that coherent (geometrical) oscillations of the maximum Josephson current are superimposed on the oscillations related to the crossovers between 0 and π states. For the same case we find that the temperature-induced 0 – π transition occurs if the junction is very close to the crossover at zero temperature.

I. INTRODUCTION

Proximity effects in superconductor (S) –ferromagnet (F) hybrid structures have been studied for some time already.¹ Recent realization of a π state in metallic SFS junctions,^{2,3,4} has reinvigorated interest in further experimental and theoretical studies.^{5,6,7,8,9,10,11,12,13,14,15,16,17,18,19,20,21,22} Nowadays, understanding of the coherent geometrical effects in ballistic heterojunctions is also becoming more important,^{23,24,25,26} due to the progress in nanofabrication technology and the improvement of experimental techniques.^{27,28,29}

The possibility of a π state in superconductors coupled through a magnetically active material (an insulating barrier containing paramagnetic impurities, or a ferromagnetic metal) has been proposed long ago.^{30,31} In the π state of an SFS structure, in contrast to the usual (0) state, the phase shift equal to π across the junction in the ground state reverses the direction of the supercurrent flow,² and drastically changes the density of states (DOS) in F metal.⁴ Following the theoretical prediction,^{32,33} an evidence for π states in proximity-coupled S-F superlattices has been sought previously in the oscillations of the superconducting critical temperature T_c as a function of the F-layers thickness.^{34,35} More recently, π states have been observed in nonmagnetic junctions of high- T_c superconductors³⁶ and in out-of-equilibrium mesoscopic superconducting structures.³⁷

Oscillations of the maximum Josephson current I_c and of the local DOS, with thickness and strength of the F layer, are prominent features of SFS metallic junctions. These oscillations are related to the crossovers between 0 and π states, the I_c minima being located at the crossover points.⁷ Nonmonotonic temperature variation of I_c , also related to the transition from π to 0 state, has been observed recently.² This effect is studied theoretically for superconducting junctions with different barriers, such as magnetically active insulating interfaces,^{8,9} metallic FIF layers (including insulating inhomogeneity and nonuniform magnetization),^{10,11,12,13,14} and ferromagnetic-metal barriers with mesoscopic disorder.¹⁵ The temperature induced 0 – π transition is attributed to the spin discrimination of Andreev bound states in the case of finite transparency and strong ferromagnetic influence.⁹

Another characteristic feature is a strong contribution of higher harmonics to the current-phase relation $I(\phi)$ in the vicinity of the crossover points, as has been shown for metallic SFS junctions in both clean and diffusive limits,^{16,17} for Josephson junctions with magnetically active insulating interface,^{9,43} and for non-equilibrium supercurrent through mesoscopic ferromagnetic weak links.¹⁸ This implies that the energy of the junction in the vicinity of the crossover has two minima as a function of ϕ , at $\phi = 0$ and $\phi = \pi$. The resulting coexistence of stable and metastable 0 and π states in the crossover region can generate two flux jumps per one external flux quantum in SQUIDs.¹⁶

The underlying microscopic mechanism is well understood. The Andreev process, recognized as the mechanism of normal-to-supercurrent conversion,^{38,39,40,41} is modified at F-S interfaces due to the spin imbalance in the ferromagnet.⁴² As a result, the superconducting pair amplitude induced in F by the proximity to S is spatially modulated.¹⁹ The current-carrying Andreev bound states are split and shifted in an oscillatory way under the influence of the ferromagnet.²⁰ The crossovers between 0 and π states and highly nonsinusoidal current-phase relation follow from the strong spin polarization of the Andreev states.^{9,43}

Several quantities characterizing the proximity effect, such as $I(\phi)$ and local DOS, have been studied in a number of theoretical works for different geometries of S-F structures, using the quasiclassical approach in both clean and

diffusive limits.^{12,13,20,21,22} However, a theory of the phase-coherent electronic transport in mesoscopic structures should be based on the solutions of Gor'kov or Bogoliubov-de Gennes (BdG) equations. The coherence effects have been studied recently for double-barrier SINIS junctions containing an interlayer of a clean nonmagnetic metal (N) with insulating interfaces (I),²³ and for FISIF junctions.^{25,26}

In this paper, we study the simultaneous influence of two insulating barriers on the supercurrent flow in ballistic double-barrier SIFIS planar junctions. The influence of different band-widths in two metals (the Fermi wave vector mismatch – FWVM) is also included. We limit ourselves to conventional (*s*-wave) superconductors. Assuming a constant pair potential in the S electrodes, we solve analytically the scattering problem based on the BdG equations, and derive a general expression for the Josephson current. This approach has been applied previously to SIS and FIS junctions with magnetically active insulating interface, both for the *s*-wave and for an unconventional pairing symmetry in superconductors.^{43,44,45} In a limiting case, our expression gives a generalization of the previous formulae for the Josephson current,^{46,47} that includes the finite interfacial transparency in SINIS junctions. Strong geometrical oscillations of I_c in the junctions with thin normal-metal interlayers and finite interfacial transparency are related to the contribution of quasiparticle transmission resonances.⁴⁸ For thin layers of a strong ferromagnet, these oscillations are superimposed on the oscillations related to the crossovers between 0 and π states. Lower transparency and FWVM shift the crossover points and narrow the adjacent regions of coexisting 0 and π states with highly nonsinusoidal current-phase relation. In a junction with finite transparency, with or without FWVM, and with strong ferromagnetic influence, the temperature-induced transition between 0 and π states occurs if the junction is sufficiently close to the crossover at zero temperature. In that case, the transition region of coexisting 0 and π states is considerably large.

The paper is organized as follows. In Sec. II, the scattering problem based on the BdG equations is solved analytically for a planar SIFIS junction, and general expressions for both the Andreev and the normal reflection amplitudes are presented. In Sec. III, an expression for the Josephson current is derived; this section includes an analysis of the influence of the junction parameters on the crossovers between 0 and π states and on the current-phase relation. Concluding remarks are given in Sec. IV.

II. THE SCATTERING PROBLEM

We consider the following model for a planar double-barrier SIFIS junction: a ferromagnetic layer of thickness d is connected to superconductors by insulating nonmagnetic interfaces. We assume that both metals are clean, that the left (L) and the right (R) superconductors are equal, and so are the interface barriers. We use the Stoner model for the ferromagnet (a uniform magnetization is parallel to the layers), and describe the quasiparticle propagation by the Bogoliubov-de Gennes equation

$$\begin{pmatrix} H_0(\mathbf{r}) - \rho_\sigma h(\mathbf{r}) & \Delta(\mathbf{r}) \\ \Delta^*(\mathbf{r}) & -H_0(\mathbf{r}) + \rho_{\bar{\sigma}} h(\mathbf{r}) \end{pmatrix} \begin{pmatrix} u_\sigma(\mathbf{r}) \\ v_{\bar{\sigma}}(\mathbf{r}) \end{pmatrix} = E \begin{pmatrix} u_\sigma(\mathbf{r}) \\ v_{\bar{\sigma}}(\mathbf{r}) \end{pmatrix}. \quad (1)$$

Here, $H_0(\mathbf{r}) = -\hbar^2 \nabla^2 / 2m + W(\mathbf{r}) + U(\mathbf{r}) - \mu$, where $U(\mathbf{r})$ and μ are the electrostatic and the chemical potential, respectively. The interface potential is modelled by $W(\mathbf{r}) = \hat{W}[\delta(z) + \delta(z - d)]$, where the z axis is perpendicular to the layers, and $\delta(z)$ is the Dirac δ -function. In Eq. (1), σ denotes the spin orientation ($\sigma = \uparrow, \downarrow$), $\bar{\sigma}$ is opposite to σ , E is the quasiparticle energy with respect to μ , $h(\mathbf{r}) = \hbar \Theta(z) \Theta(d - z)$ is the exchange potential, where $\Theta(z)$ is the Heaviside step function, and ρ_σ is 1 (−1) for $\sigma = \uparrow$ (\downarrow). Neglecting the self-consistency of the superconducting pair potential, $\Delta(\mathbf{r})$ is taken in the form

$$\Delta(\mathbf{r}) = \Delta [e^{i\phi_L} \Theta(-z) + e^{i\phi_R} \Theta(z - d)], \quad (2)$$

where Δ is the bulk superconducting gap, and $\phi = \phi_R - \phi_L$ is the macroscopic phase difference across the junction. The temperature dependence of Δ is given by $\Delta(T) = \Delta(0) \tanh \left(1.74 \sqrt{T_c/T - 1} \right)$. The electron effective mass m is assumed to be the same for both metals, $\mu - U(\mathbf{r})$ is the Fermi energy of the superconductor, $E_F^{(S)}$, or the mean Fermi energy of the ferromagnet, $E_F^{(F)} = (E_F^\uparrow + E_F^\downarrow)/2$. Moduli of the Fermi wave vectors, $k_F^{(S)} = \sqrt{2mE_F^{(S)}/\hbar^2}$ and $k_F^{(F)} = \sqrt{2mE_F^{(F)}/\hbar^2}$, may be different in general, and in the following the FWVM will be parameterized by $\kappa = k_F^{(F)}/k_F^{(S)}$.

The parallel component of the wave vector \mathbf{k}_\parallel is conserved, and the wave function

$$\begin{pmatrix} u_\sigma(\mathbf{r}) \\ v_{\bar{\sigma}}(\mathbf{r}) \end{pmatrix} = \exp(i\mathbf{k}_\parallel \cdot \mathbf{r}) \psi(z) \quad (3)$$

satisfies appropriate boundary conditions

$$\psi(z)|_{z=0_-} = \psi(z)|_{z=0_+}, \quad (4)$$

$$\left. \frac{d\psi(z)}{dz} \right|_{z=0_-} = \left. \frac{d\psi(z)}{dz} \right|_{z=0_+} - \frac{2m\hat{W}}{\hbar^2} \psi(0), \quad (5)$$

$$\psi(z)|_{z=d_-} = \psi(z)|_{z=d_+}, \quad (6)$$

$$\left. \frac{d\psi(z)}{dz} \right|_{z=d_-} = \left. \frac{d\psi(z)}{dz} \right|_{z=d_+} - \frac{2m\hat{W}}{\hbar^2} \psi(d). \quad (7)$$

The four independent solutions of Eq. (1) correspond to four types of quasiparticle injection processes: an electron-like quasiparticle (ELQ) or a hole-like quasiparticle (HLQ) injected from either the left or from the right superconducting electrode (see Fig. 2 in Ref.⁴⁰).

For the injection of an ELQ from the left superconductor with energy $E > \Delta$ and angle of incidence θ (measured from the z -axis), $\psi(z)$ has the following form

$$\psi_1(z) = \begin{cases} [\exp(ik^+z) + b_1 \exp(-ik^+z)] \begin{pmatrix} \bar{u}e^{i\phi_L/2} \\ \bar{v}e^{-i\phi_L/2} \end{pmatrix} + a_1 \exp(ik^-z) \begin{pmatrix} \bar{v}e^{i\phi_L/2} \\ \bar{u}e^{-i\phi_L/2} \end{pmatrix} & z < 0, \\ [C_1 \exp(iq_\sigma^+z) + C_2 \exp(-iq_\sigma^+z)] \begin{pmatrix} 1 \\ 0 \end{pmatrix} + [C_3 \exp(iq_\sigma^-z) + C_4 \exp(-iq_\sigma^-z)] \begin{pmatrix} 0 \\ 1 \end{pmatrix} & 0 < z < d, \\ c_1 \exp(ik^+z) \begin{pmatrix} \bar{u}e^{i\phi_R/2} \\ \bar{v}e^{-i\phi_R/2} \end{pmatrix} + d_1 \exp(-ik^-z) \begin{pmatrix} \bar{v}e^{i\phi_R/2} \\ \bar{u}e^{-i\phi_R/2} \end{pmatrix} & z > d. \end{cases} \quad (8)$$

Here, $\bar{u} = \sqrt{(1 + \Omega/E)/2}$ and $\bar{v} = \sqrt{(1 - \Omega/E)/2}$ are the BCS amplitudes, and $\Omega = \sqrt{E^2 - \Delta^2}$. Perpendicular (z) components of the wave vectors are

$$k^\pm = \left[(2m/\hbar^2)(E_F^{(S)} \pm \Omega) - \mathbf{k}_\parallel^2 \right]^{1/2}, \quad (9)$$

and

$$q_\sigma^\pm = \left[(2m/\hbar^2)(E_F^{(F)} + \rho_\sigma \hbar \pm E) - \mathbf{k}_\parallel^2 \right]^{1/2}, \quad (10)$$

where $|\mathbf{k}_\parallel| = \sqrt{(2m/\hbar^2)(E_F^{(S)} + \Omega)} \sin \theta$ is the conserved parallel component. The coefficients a_1 , b_1 , c_1 , and d_1 are, respectively, the probability amplitudes of the generalized Andreev reflection as a HLQ, normal reflection as an ELQ, transmission to the right electrode as an ELQ, and transmission to the right electrode as an HLQ.⁴⁰ Amplitudes of electrons and holes propagating in the ferromagnetic layer are given by the coefficients C_1 through C_4 . All amplitudes are σ -dependent through the Zeeman terms in q_σ^\pm , but there is no spin current across the junction in contrast to FIS and FISIF geometry.^{26,42,45} ELQ and the Andreev-reflected HLQ have identical spin orientations in absence of spin-flip processes and for singlet-state pairing in SIFIS geometry.¹⁴

For the injection of a HLQ from the left superconductor with energy $E > \Delta$ and angle of incidence θ , $\psi(z)$ is

$$\psi_2(z) = \begin{cases} [\exp(-ik^-z) + b_2 \exp(ik^-z)] \begin{pmatrix} \bar{v}e^{i\phi_L/2} \\ \bar{u}e^{-i\phi_L/2} \end{pmatrix} + a_2 \exp(-ik^+z) \begin{pmatrix} \bar{u}e^{i\phi_L/2} \\ \bar{v}e^{-i\phi_L/2} \end{pmatrix} & z < 0, \\ [C'_1 \exp(iq_\sigma^+z) + C'_2 \exp(-iq_\sigma^+z)] \begin{pmatrix} 1 \\ 0 \end{pmatrix} + [C'_3 \exp(iq_\sigma^-z) + C'_4 \exp(-iq_\sigma^-z)] \begin{pmatrix} 0 \\ 1 \end{pmatrix} & 0 < z < d \\ c_2 \exp(-ik^-z) \begin{pmatrix} \bar{v}e^{i\phi_R/2} \\ \bar{u}e^{-i\phi_R/2} \end{pmatrix} + d_2 \exp(ik^+z) \begin{pmatrix} \bar{u}e^{i\phi_R/2} \\ \bar{v}e^{-i\phi_R/2} \end{pmatrix} & z > d, \end{cases} \quad (11)$$

where the wave vectors are given by Eqs. (9) and (10), with $|\mathbf{k}_\parallel| = \sqrt{(2m/\hbar^2)(E_F^{(S)} - \Omega)} \sin \theta$. Analogously, one can write ψ_3 and ψ_4 for an injection of ELQ and HLQ from the right superconductor, respectively.

Solutions of Eqs. (4)–(7) for the scattering amplitudes can be simplified significantly if one neglects, except in exponentials, small terms $\Omega/E_F^{(S)} \ll 1$ and $E/E_F^{(F)} \ll 1$ in the wave vectors. In the following, $|\mathbf{k}_\parallel| = k_F^{(S)} \sin \theta$, the

wave vectors k^\pm are replaced by $k = \sqrt{k_F^{(S)^2} - \mathbf{k}_\parallel^2} = k_F^{(S)} \cos \theta$, and in the pre-exponential factors only, q_σ^+ and $q_{\bar{\sigma}}^-$ are replaced by q_σ and $q_{\bar{\sigma}}$, where $q_\sigma = \sqrt{k_F^{(F)^2} (1 + \rho_\sigma h / E_F^{(F)}) - \mathbf{k}_\parallel^2}$. Physically important oscillations of the scattering amplitudes, both rapid and slow on the atomic scale $1/k_F^{(F)}$, are characterized respectively by the exponents

$$\zeta_\sigma^\pm = d (q_\sigma^\pm \pm q_{\bar{\sigma}}^\mp). \quad (12)$$

First we present the results for a_1 and b_1 , given by

$$a_1 = \frac{2\Delta}{G} [-4\tilde{q}_\sigma \tilde{q}_{\bar{\sigma}} (E \cos \phi + i\Omega \sin \phi) + \mathcal{A}_1^- \cos(\zeta_\sigma^-) - \mathcal{A}_1^+ \cos(\zeta_\sigma^+) - i\mathcal{A}_2^- \sin(\zeta_\sigma^-) + i\mathcal{A}_2^+ \sin(\zeta_\sigma^+)], \quad (13)$$

and

$$b_1 = \frac{2\Omega}{G} [\mathcal{B}_1^- \cos(\zeta_\sigma^-) - \mathcal{B}_1^+ \cos(\zeta_\sigma^+) - i\mathcal{B}_2^- \sin(\zeta_\sigma^-) + i\mathcal{B}_2^+ \sin(\zeta_\sigma^+)], \quad (14)$$

where

$$\begin{aligned} \mathcal{A}_1^\pm &= (\tilde{q}_\sigma \mp \tilde{q}_{\bar{\sigma}}) [E (\tilde{q}_\sigma \mp \tilde{q}_{\bar{\sigma}}) - i\Omega Z_\theta (\tilde{q}_\sigma \pm \tilde{q}_{\bar{\sigma}})], \\ \mathcal{A}_2^\pm &= \Omega (\tilde{q}_\sigma \mp \tilde{q}_{\bar{\sigma}}) [1 + Z_\theta^2 \mp \tilde{q}_\sigma \tilde{q}_{\bar{\sigma}}], \end{aligned} \quad (15)$$

and

$$\begin{aligned} \mathcal{B}_1^\pm &= E (1 - iZ_\theta) [(\tilde{q}_\sigma)^2 - (\tilde{q}_{\bar{\sigma}})^2] \\ &\quad - \Omega \left\{ (1 + Z_\theta^2) (1 - iZ_\theta)^2 - (\tilde{q}_\sigma)^2 (\tilde{q}_{\bar{\sigma}})^2 + iZ_\theta (1 - iZ_\theta) [(\tilde{q}_\sigma)^2 \pm 4\tilde{q}_\sigma \tilde{q}_{\bar{\sigma}} + (\tilde{q}_{\bar{\sigma}})^2] \right\}, \\ \mathcal{B}_2^\pm &= -E (\tilde{q}_\sigma \mp \tilde{q}_{\bar{\sigma}}) [(1 - iZ_\theta)^2 \pm \tilde{q}_\sigma \tilde{q}_{\bar{\sigma}}] \\ &\quad + \Omega (\tilde{q}_\sigma \pm \tilde{q}_{\bar{\sigma}}) [(1 + 2iZ_\theta) (1 - iZ_\theta)^2 \mp (1 - 2iZ_\theta) \tilde{q}_\sigma \tilde{q}_{\bar{\sigma}}]. \end{aligned} \quad (16)$$

The common denominator is given by

$$G = 8\Delta^2 \tilde{q}_\sigma \tilde{q}_{\bar{\sigma}} \cos \phi - \mathcal{G}_1^- \cos(\zeta_\sigma^-) + \mathcal{G}_1^+ \cos(\zeta_\sigma^+) + i\mathcal{G}_2^- \sin(\zeta_\sigma^-) - i\mathcal{G}_2^+ \sin(\zeta_\sigma^+), \quad (17)$$

where

$$\begin{aligned} \mathcal{G}_1^\pm &= \left\{ E (\tilde{q}_\sigma \mp \tilde{q}_{\bar{\sigma}}) + \Omega [1 + Z_\theta^2 - iZ_\theta (\tilde{q}_\sigma \pm \tilde{q}_{\bar{\sigma}}) \mp \tilde{q}_\sigma \tilde{q}_{\bar{\sigma}}] \right\}^2 \\ &\quad + \left\{ E (\tilde{q}_\sigma \mp \tilde{q}_{\bar{\sigma}}) - \Omega [1 + Z_\theta^2 + iZ_\theta (\tilde{q}_\sigma \pm \tilde{q}_{\bar{\sigma}}) \mp \tilde{q}_\sigma \tilde{q}_{\bar{\sigma}}] \right\}^2, \\ \mathcal{G}_2^\pm &= 4\Omega (1 + Z_\theta^2 \mp \tilde{q}_\sigma \tilde{q}_{\bar{\sigma}}) [E (\tilde{q}_\sigma \mp \tilde{q}_{\bar{\sigma}}) - i\Omega Z_\theta (\tilde{q}_\sigma \pm \tilde{q}_{\bar{\sigma}})]. \end{aligned} \quad (18)$$

Here, we introduced the normalized quantities $\tilde{q}_\sigma = q_\sigma/k$, and $Z_\theta = Z/\cos \theta$, where $Z = 2m\hat{W}/\hbar^2 k_F^{(S)}$ is the parameter measuring the strength of each insulating interface. Note that all amplitudes are functions of E , σ , θ , and ϕ , for given Δ , h , and Z .

The Andreev reflection amplitudes a_2 and a_1 are simply connected. For the same E , σ and θ in our approximation we get

$$a_2(\phi) = a_1(-\phi), \quad (19)$$

which is in agreement with the detailed balance relations.⁴⁰ Expression for b_2 can be given in a form similar to b_1 , so that

$$b_2 = \frac{2\Omega}{G} [\bar{\mathcal{B}}_1^- \cos(\zeta_\sigma^-) - \bar{\mathcal{B}}_1^+ \cos(\zeta_\sigma^+) + i\bar{\mathcal{B}}_2^- \sin(\zeta_\sigma^-) - i\bar{\mathcal{B}}_2^+ \sin(\zeta_\sigma^+)], \quad (20)$$

with G given by Eq. (17), and

$$\begin{aligned} \bar{\mathcal{B}}_1^\pm &= -E (1 + iZ_\theta) [(\tilde{q}_\sigma)^2 - (\tilde{q}_{\bar{\sigma}})^2] \\ &\quad - \Omega \left\{ (1 + Z_\theta^2) (1 + iZ_\theta)^2 - (\tilde{q}_\sigma)^2 (\tilde{q}_{\bar{\sigma}})^2 - iZ_\theta (1 + iZ_\theta) [(\tilde{q}_\sigma)^2 \pm 4\tilde{q}_\sigma \tilde{q}_{\bar{\sigma}} + (\tilde{q}_{\bar{\sigma}})^2] \right\}, \\ \bar{\mathcal{B}}_2^\pm &= -E (\tilde{q}_\sigma \mp \tilde{q}_{\bar{\sigma}}) [(1 + iZ_\theta)^2 \pm \tilde{q}_\sigma \tilde{q}_{\bar{\sigma}}] \\ &\quad - \Omega (\tilde{q}_\sigma \pm \tilde{q}_{\bar{\sigma}}) [(1 - 2iZ_\theta) (1 + iZ_\theta)^2 \mp (1 + 2iZ_\theta) \tilde{q}_\sigma \tilde{q}_{\bar{\sigma}}]. \end{aligned} \quad (21)$$

Note that the normal-reflection amplitudes, b_1 through b_4 , are even functions of ϕ . From the assumed symmetry of the junction, within our approximation it follows that $a_3 = a_2$, $a_4 = a_1$, $b_3 = b_1$, and $b_4 = b_2$.⁴⁹

In the corresponding NIFIN junction, when the superconductor electrodes are in the normal state, the expressions for the normal reflection amplitudes reduce to $b_1 = b_2 \equiv b_N$, where

$$b_N = \frac{2Z_\theta \tilde{q}_\sigma \cos(dq_\sigma) + (1 + Z_\theta^2 - \tilde{q}_\sigma^2) \sin(dq_\sigma)}{2i(1 + iZ_\theta) \tilde{q}_\sigma \cos(dq_\sigma) + (1 + 2iZ_\theta - Z_\theta^2 + \tilde{q}_\sigma^2) \sin(dq_\sigma)}. \quad (22)$$

Because of the conservation of \mathbf{k}_\parallel , ELQ and HLQ undergo the total reflection for $\theta > \theta_{c\sigma} = \sin^{-1} \lambda_\sigma$, if $\lambda_\sigma = \kappa \sqrt{1 + \rho_\sigma \hbar / E_F^{(F)}} < 1$. The corresponding q_σ becomes imaginary and electrons and/or holes, depending on the spin orientation, cannot propagate in the ferromagnetic layer. However, the contribution of an evanescent type of the Andreev reflection to the Josephson current is not negligible,⁴⁵ and should be taken into account in the finite geometry.

III. THE JOSEPHSON CURRENT

The dc Josephson current at a given temperature can be expressed in terms of the Andreev reflection amplitudes by using the temperature Green's function formalism⁴⁰

$$I = \frac{e\Delta}{2\hbar} \sum_{\sigma, \mathbf{k}_\parallel} k_B T \sum_{\omega_n} \frac{1}{2\Omega_n} (k_n^+ + k_n^-) \left(\frac{a_{n1}}{k_n^+} - \frac{a_{n2}}{k_n^-} \right), \quad (23)$$

where k_n^+ , k_n^- , and a_{n1} , a_{n2} are obtained from k^+ , k^- , and a_1 , a_2 by the analytic continuation $E \rightarrow i\omega_n$, the Matsubara frequencies are $\omega_n = \pi k_B T (2n + 1)$ with $n = 0, \pm 1, \pm 2, \dots$, and $\Omega_n = \sqrt{\omega_n^2 + \Delta^2}$. Performing integration over \mathbf{k}_\parallel and using Eqs. (13) and (19), for the Josephson current in a planar SIFIS junction we get

$$I = \frac{4\pi k_B T \Delta^2}{eR} \int_0^{\pi/2} d\theta \sin \theta \cos \theta \sum_{\omega_n, \sigma} \frac{\tilde{q}_\sigma \tilde{q}_{\bar{\sigma}} \sin \phi}{G_n}. \quad (24)$$

Here, G_n is G given by Eq. (17), with E and Ω replaced by $i\omega_n$ and $i\Omega_n$. Note that $R = 2\pi^2 \hbar / S e^2 k_F^{(F)^2}$, where S is the area of the junction, is the normal resistance only for $Z = 0$, $\kappa = 1$, and $h = 0$, when the normal reflection amplitude b_N is equal to zero. The resistance R_N of the corresponding NIFIN junction can be obtained from

$$\frac{R}{R_N} = \int_0^{\pi/2} d\theta \sin \theta \cos \theta \sum_{\sigma} (1 - |b_N|^2). \quad (25)$$

The spectrum of bound states in the interlayer is included in the common denominator of the retarded Green's function. For transparent nonmagnetic junctions without FWVM, when $R_N/R = 1$, the condition $G(E) = 0$ gives well-known phase-dependent and spin-degenerate Andreev bound states with subgap energies.⁴⁶ For resistive ferromagnetic junctions, when $R_N/R > 1$, the spectrum of Andreev bound states is modified by the coherent contribution of geometrical resonances in the ferromagnet (described by the rapidly oscillating terms) and by the Zeeman splitting.

For a weak ferromagnet, $\hbar/E_F^{(F)} \ll 1$, wave vectors q_σ and $q_{\bar{\sigma}}$ can both be replaced by $q = \sqrt{k_F^{(F)^2} - \mathbf{k}_\parallel^2}$, so that $\tilde{q}_\sigma, \tilde{q}_{\bar{\sigma}} \rightarrow \tilde{q} = q/k$. Also, ζ_σ^\pm can be approximated as $\zeta_\sigma^- \simeq 2d(E + \rho_\sigma \hbar)/\hbar v$ and $\zeta_\sigma^+ \simeq 2qd$, where $v = \hbar q/m$ is the z component of the Fermi velocity in the absence of FWVM. In this limit, the general formula, Eq. (24), reduces to

$$I = \frac{\pi k_B T \Delta^2}{eR} \int_0^{\pi/2} d\theta \sin \theta \cos \theta \sum_{\omega_n} \frac{1}{2} \sum_{\sigma} \frac{\sin \phi}{\Gamma_n}, \quad (26)$$

with

$$\begin{aligned} \Gamma_n = & \Delta^2 \cos \phi + (K^2 \Omega_n^2 + \omega_n^2) \cosh \left[\frac{2(\omega_n - i\rho_\sigma \hbar)d}{\hbar v} \right] + 2K\omega_n \Omega_n \sinh \left[\frac{2(\omega_n - i\rho_\sigma \hbar)d}{\hbar v} \right] \\ & - (K^2 - 1 - 2Z_\theta^2) \Omega_n^2 \cos(2qd) + 2Z_\theta (K^2 - 1 - Z_\theta^2)^{1/2} \Omega_n^2 \sin(2qd), \end{aligned} \quad (27)$$

where

$$K = \frac{1}{2} \left(\tilde{q} + \frac{1 + Z_{\theta}^2}{\tilde{q}} \right). \quad (28)$$

We emphasize that the obtained expressions are consistent with previous formulae for the Josephson current. For $h = 0$, Eqs. (26)–(28) are generalization of the Furusaki-Tsukada formula⁴⁶ to double-barrier SINIS junctions with $Z \neq 0$. For equal Fermi energies of the two metals and for transparent interfaces, $\kappa = 1$ and $Z = 0$, the rapidly oscillating terms are absent, and Eq. (26) reduces to the well known quasiclassical expression in the clean limit.^{16,31} In Eq. (27), a weak exchange potential is taken into account only by its contribution to the phase of the superconducting pair potential, $-i\rho_{\sigma}hd/\hbar v$ in sinh and cosh terms, that implies oscillations of $I(\phi)$ and changes the sign of the current at the crossovers between 0 and π states. For $k_B T_c \ll \hbar/E_F^{(F)} < 0.1$, the current-phase relation is almost a universal function of the parameter $\Theta = (k_F^{(F)}d)(\hbar/E_F^{(F)})$, which measures the total influence of the ferromagnet. For a stronger ferromagnet this is not the case, and the general Eq. (24) has to be applied. In all illustrations (Figs. 1 – 6) we have used Eq. (24), characterizing superconductors with $\Delta/E_F^{(S)} = 10^{-3}$.

Characteristic feature of the ballistic SIFIS junctions is an oscillatory dependence of $I(\phi)$ and I_c on h and d , which is related to the crossovers between 0 and π states. However, even in SINIS junctions (where 0 state is the equilibrium one) geometrical oscillations of the supercurrent occur due to the coherent contribution of the quasiparticle transmission resonances.^{23,48} To stress this effect, in Fig. 1 we show an example of a thin and weak ferromagnet, $\hbar/E_F^{(F)} = 0.01$, and compare it to a nonmagnetic-metal interlayer, $h = 0$, for the same interfacial transparency, $Z = 1$, at low temperature $T/T_c = 0.1$. In this case, geometrical oscillations are dominant, the SIFIS junction being also in the 0 state (the first crossover from 0 to π state occurs for $dk_F^{(F)} = 125$).

The interplay between geometrical oscillations and those induced by a strong exchange potential is shown in Fig. 2 for thin ferromagnetic layers with $\hbar/E_F^{(F)} = 0.9$. Oscillations of $I_c(d)$ due to the exchange potential are shown in Fig. 2(a) for a junction with transparent interfaces, $Z = 0$, equal Fermi energies, $\kappa = 1$, and for two temperatures. For finite interfacial transparency, $Z = 1$, these oscillations are superimposed on the geometrical ones, Fig. 2(b). In the same figure, the influence of different band-widths in S and F metals is also shown for $\kappa = 0.7$. Here, we use the normalization $I_c R$, instead of $I_c R_N$ used in Fig. 1, to clearly show the influence of the junction parameters (h , d , Z , and κ) on the maximum supercurrent. Mean values of the normal resistance corresponding, for example, to solid curves in Figs. 2(a) and 2(b) are $R_N/R = 2.34$ and 4.55 , respectively.

The characteristic variation of nonsinusoidal $I(\phi)$ in the vicinity of the crossover between 0 and π states is illustrated in Fig. 3 for a highly resistive junction with the same parameters used in Fig. 2(b), solid curve. Lower transparency and FWVM, $Z = 1$ and $\kappa = 0.7$, shift the crossover point at $T/T_c = 0.1$ from $d_c = 9.45/k_F^{(F)}$ in a transparent junction (second dip of solid curve in Fig. 2(a)) to $d_c = 8.72/k_F^{(F)}$ (second dip of solid curve in Fig. 2(b)). The region of coexisting 0 and π states, $8.63 < dk_F^{(F)} < 8.82$, is two times narrower than that in the transparent junction, $9.2 < dk_F^{(F)} < 9.6$. With increase of temperature or decrease of transparency the contribution from the higher-order scattering processes becomes negligible, transition regions become narrower and $I(\phi)$ approaches the ordinary sinusoidal dependence, $\pm I_c \sin \phi$, where \pm correspond to 0 and π junction, respectively. Note that similar highly nonsinusoidal variation of $I(\phi)$ also occurs in SF-FS Josephson junctions with transparent geometrical constrictions.¹⁷ However, such a behavior is not stable against a disorder. In diffusive double-barrier SIFIS junctions $I(\phi)$ does not cross the ϕ axis in the interval between 0 and π .¹⁷

The temperature variation of I_c is usually a monotonic decay with increasing temperature. However, depending on parameters of the junction, the transition between 0 and π states can be induced by changing the temperature. In that case, I_c manifests nonmonotonic dependence on temperature with a well-pronounced dip at the transition. This is illustrated in Fig. 4 for the SIFIS junctions with $\hbar/E_F^{(F)} = 0.92$, $Z = 1.2$, $\kappa = 1$, and three values of d close to $d_c = 17.27/k_F^{(F)}$ at zero temperature ($d_c = 17.14/k_F^{(F)}$ at $T = 0.9T_c$). Three characteristic $I_c(T)$ curves are shown for $dk_F^{(F)} = 17$ (0 state), 17.4 (π state), and 17.23 (the temperature increase induces a transition from 0 to π state at $T/T_c = 0.22$). A considerably large transition region of coexisting 0 and π states, $0.1 < T/T_c < 0.3$, is shown in Fig. 5. Similar 0 – π transitions occur at different temperatures in a very narrow region $17.2 < dk_F^{(F)} < 17.3$ about the crossover d_c at zero temperature. We emphasize that the temperature-induced transition takes place in the vicinity of any crossover point of the junctions with finite transparency, with or without FWVM, and with strong ferromagnetic influence. For example, the temperature-induced transitions occur in the vicinity of the crossover points in Fig. 2(b), represented by dips in both solid and dotted $I_c(d)$ curves. However, this is not the case for transparent interfaces, for example in the vicinity of dips in solid $I_c(d)$ curve in Fig. 2(a). These results are in agreement with the general conditions for the occurrence of the temperature induced 0 – π transition, given in Ref.⁹.

For thick layers of a weak ferromagnet, $\hbar/E_F^{(F)} = 0.01$, oscillations of $I_c(d)$ due to the exchange potential are shown

in Fig. 6(a) for a junction with transparent interfaces, $Z = 0$, equal Fermi energies, $\kappa = 1$, and for two temperatures. The influence of interfacial resistance and of FWVM at low temperature is illustrated in Fig. 6(b). One can see that the contribution of geometrical resonances is negligible in that case. Oscillations of $I_c(d)$ in the resistive junctions ($R_N/R = 5, 2.5$, and 2.2 for solid, dotted, and dashed curves in Fig. 6(b), respectively) are similar to those in the non-resistive one, Fig. 6(a), with shifted d_c and significant lowering of amplitudes. However, regions of coexisting 0 and π states are considerably narrower in the resistive junctions. For example, at low temperature, $T/T_c = 0.1$, in a junction with transparent interfaces and without FWVM, the crossover from 0 to π state occurs at $d_c k_F^{(F)} = 111$ (first dip in solid curve, Fig. 6(a)) with coexisting 0 and π states in the region $60 < dk_F^{(F)} < 130$, while in a junction with finite transparency and FWVM ($Z = 1, \kappa = 0.7$), the corresponding crossover occurs at $d_c k_F^{(F)} = 120$ (first dip in solid curve, Fig. 6(b)), and the coexisting region, $110 < dk_F^{(F)} < 125$, is five times narrower. Because of weak ferromagnetic influence the temperature-induced transition is not found for the parameters displayed in Fig. 6.

IV. CONCLUDING REMARKS

We have derived an expression for the Josephson current in planar ballistic SIFS junctions, generalizing the Furusaki - Tsukada formula⁴⁶ so that it includes interfacial non-transparency and ferromagnetism in the normal-metal interlayer. We used a non-self-consistent step function for the pair potential, but in the case of low transparency, FWVM, and/or thin interlayers, our results will not be altered significantly. In that case, the depletion of the pair potential in the superconductors is negligible. Characteristic proximity effects at transparent FS interfaces have to be studied by a self-consistent numerical treatment.¹⁹ In order to obtain simpler expressions for the scattering amplitudes, we have neglected, except in exponentials, the small energy terms in the wave vectors, since their contribution is typically less than 0.1%. These terms are not neglected, however, in the exponentials, so that we take into account the significant contribution from both resonant and bound states, represented by rapidly and slowly oscillating terms.

The solutions obtained for the Andreev and the normal reflection amplitudes provide a fully microscopic study of the coherent superconducting properties in ballistic double-barrier junctions with ferromagnetic, or nonmagnetic normal-metal interlayer. The resulting wave functions and the quasiparticle excitation energies can be used to compute all physically relevant quantities, e.g. the local DOS and the superconducting pair amplitude.⁴⁹ These applications of our results are left for future work.

Qualitatively, our results confirm previously obtained main features of the metallic SFS systems, and uncover new coherency effects in nanostructured ballistic junctions. The pronounced geometrical oscillations of the supercurrent occur in double-barrier SINIS junctions with thin interlayers of a clean normal metal, due to the coherent contribution of the quasiparticle transmission resonances to the Andreev bound states.⁴⁸ The amplitudes of the supercurrent oscillations are significantly larger than those of the normal current in the corresponding NININ ballistic junction. For thin layer of a strong ferromagnet, we found that geometrical oscillations are superimposed on the oscillations induced by crossovers between 0 and π states. For high interfacial transparency and/or thick interlayers, coherency effects are less pronounced, in agreement with previous theoretical results.²³ Low interfacial transparency and FWVM affect the position of crossover points, and narrower the transition regions of coexisting 0 and π states.

We have shown that the temperature induced transition occurs in ballistic SIFS junctions with finite interfacial transparency and strong ferromagnetic influence, if the parameters of the junction are sufficiently close to the crossover at zero temperature. The characteristic nonmonotonic variation of the maximum Josephson current with temperature agrees with previous experimental and theoretical results.^{2,8,9,10,11,12,13,14,15} However, in the ballistic junctions the transition region of coexisting 0 and π states is considerably large. This effect can be exploited, for example, in the design of a π SQUID with improved accuracy, which operates as a usual one with effectively two times smaller flux quantum.¹⁶ Such a device has potential applications in novel quantum electronics.⁵⁰

V. ACKNOWLEDGMENTS

The work was supported in part by the Greek-Yugoslav Scientific and Technical Cooperation program on Superconducting Heterostructures and Devices. Z. R. acknowledges also the support of the Serbian Ministry of Science, Technology and Development, Project No. 1899, and thanks Ivan Božović and Miloš Božović for useful discussions.

¹ P. M. Tedrow and R. Meservey, Phys. Rep. **238**, 173 (1994).

- ² V. V. Ryazanov, V. A. Oboznov, A. Yu. Rusanov, A. V. Veretennikov, A. A. Golubov, and J. Aarts, Phys. Rev. Lett. **86**, 2427 (2001).
- ³ V. V. Ryazanov, V. A. Oboznov, A. V. Veretennikov, and A. Yu. Rusanov, Phys. Rev. B **65**, 020501 (2001).
- ⁴ T. Kontos, M. Aprili, J. Lesueur, and X. Grisson, Phys. Rev. Lett. **86**, 304 (2001).
- ⁵ J. M. E. Geers, M. B. S. Hesselberth, J. Aarts, and A. A. Golubov, Phys. Rev. B **64**, 094506 (2001).
- ⁶ O. Bourgeois, P. Gandit, J. Lesueur, A. Sulpice, X. Grisson, and J. Chaussy, Eur. Phys. J. B **21**, 75 (2001).
- ⁷ T. Kontos, M. Aprili, J. Lesueur, F. Genêt, B. Stephanidis, and R. Boursier, Phys. Rev. Lett. **89**, 137007 (2002).
- ⁸ M. Fogelström, Phys. Rev. B **62**, 11812 (2000).
- ⁹ Yu. S. Barash and I. V. Bobkova, Phys. Rev. B **65**, 144502 (2002).
- ¹⁰ N. M. Chtchelkatchev, W. Belzig, Yu. V. Nazarov, and C. Bruder, Pis'ma Zh. Éksp. Teor. Fiz. **74**, 357 (2001) [JETP Lett. **74**, 323 (2001)].
- ¹¹ V. N. Krivoruchko and E. A. Koshina, Phys. Rev. B **64**, 172511 (2001).
- ¹² F. S. Bergeret, A. F. Volkov, and K. B. Efetov, Phys. Rev. B **64**, 134506 (2001).
- ¹³ A. A. Golubov, M. Yu. Kupriyanov, and Ya. V. Fominov, Pis'ma Zh. Éksp. Teor. Fiz. **75**, 223 (2002) [JETP Lett. **75**, 190 (2002)].
- ¹⁴ Yu. S. Barash, I. V. Bobkova, and T. Kopp, Phys. Rev. B **66**, 140503 (2002).
- ¹⁵ A. Yu. Zyuzin, B. Spivak, and M. Hruška, Europhys. Lett. **62**, 97 (2003).
- ¹⁶ Z. Radović, L. Dobrosavljević-Grujić, and B. Vujičić, Phys. Rev. B **63**, 214512 (2001).
- ¹⁷ A. A. Golubov, M. Yu. Kupriyanov, and Ya. V. Fominov, Pis'ma Zh. Éksp. Teor. Fiz. **75**, 588 (2002) [JETP Lett. **75**, 709 (2002)].
- ¹⁸ T. T. Heikkilä, F. K. Wilhelm, and G. Schön, Europhys. Lett. **51**, 434 (2000).
- ¹⁹ K. Halterman and O. T. Valls, Phys. Rev. B **65**, 014509 (2001); **66**, 224516 (2002).
- ²⁰ M. Zareyan, W. Belzig, and Yu. V. Nazarov, Phys. Rev. Lett. **86**, 308 (2001).
- ²¹ I. Baladie and A. Buzdin, Phys. Rev. B **64**, 224514 (2001).
- ²² F. S. Bergeret, A. F. Volkov, and K. B. Efetov, Phys. Rev. B **65**, 134505 (2002).
- ²³ A. Brinkman and A. A. Golubov, Phys. Rev. B **61**, 11297 (2000).
- ²⁴ A. Ingerman, G. Johansson, V. S. Shumeiko, and G. Wendin, Phys. Rev. B **64**, 144504 (2001).
- ²⁵ K. Kikuchi, H. Imamura, S. Takahashi, and S. Maekawa, Phys. Rev. B **65**, 020508 (2001).
- ²⁶ M. Božović and Z. Radović, Phys. Rev. B **66**, 134524 (2002).
- ²⁷ I. P. Nevirkovets, J. B. Ketterson, and S. Lomatch, Appl. Phys. Lett. **74**, 1624 (1999).
- ²⁸ H. Schulze, R. Behr, F. Müller, and J. Niemeyer, Appl. Phys. Lett. **73**, 996 (1998).
- ²⁹ N. Moussy, H. Courtois, and B. Pannetier, Rev. Sci. Instrum. **72**, 128 (2002).
- ³⁰ L. N. Bulaevskii, V. V. Kuzii, and A. A. Sobyenin, Pis'ma Zh. Éksp. Teor. Fiz. **25**, 314 (1977) [JETP Lett. **25**, 290 (1977)].
- ³¹ A. I. Buzdin, L. N. Bulaevskii, and S. V. Paniukov, Pis'ma Zh. Éksp. Teor. Fiz. **35**, 147 (1982) [JETP Lett. **35**, 178 (1982)].
- ³² Z. Radović, M. Ledvij, Lj. Dobrosavljević-Grujić, A. I. Buzdin, and J. R. Clem, Phys. Rev. B **44**, 759 (1991).
- ³³ A. I. Buzdin and M. V. Kupriyanov, Pis'ma Zh. Éksp. Teor. Fiz. **52**, 1089, (1990) [JETP Lett. **52**, 487 (1990)].
- ³⁴ J. S. Jiang, D. Davidović, D. H. Reich, and C. L. Chien, Phys. Rev. Lett. **74**, 314 (1995).
- ³⁵ Y. Obi, M. Ikebe, T. Kubo, and H. Fujimori, Physica C **317-318**, 149 (1999).
- ³⁶ D. J. van Harlingen, Rev. Mod. Phys. **67**, 515 (1995).
- ³⁷ J. J. A. Baselmans, T. T. Heikkilä, B. J. van Wees, and T. M. Klapwijk, Phys. Rev. Lett. **89**, 207002 (2002); J. J. A. Baselmans, A. F. Morpurgo, B. J. van Wees, and T. M. Klapwijk, Nature (London) **397**, 43 (1999).
- ³⁸ A. F. Andreev, Zh. Eksp. Teor. Fiz. **46**, 1823 (1964) [Sov. Phys. JETP **19**, 1228 (1964)].
- ³⁹ G. E. Blonder, M. Tinkham, and T. M. Klapwijk, Phys. Rev. B **25**, 4515 (1982).
- ⁴⁰ A. Furusaki and M. Tsukada, Solid State Commun. **78**, 299 (1991).
- ⁴¹ C. W. J. Beenakker, Phys. Rev. Lett. **67**, 3836 (1991).
- ⁴² M. J. M. de Jong and C. W. J. Beenakker, Phys. Rev. Lett. **74**, 1657 (1995).
- ⁴³ Y. Tanaka and S. Kashiwaya, Physica C **274**, 357 (1997).
- ⁴⁴ Y. Tanaka and S. Kashiwaya, J. Phys. Soc. Japan **69**, 1152 (2000).
- ⁴⁵ S. Kashiwaya, Y. Tanaka, N. Yoshida, and M. R. Beasley, Phys. Rev. B **60**, 3572 (1999).
- ⁴⁶ A. Furusaki and M. Tsukada, Phys. Rev. B **43**, 10164 (1991).
- ⁴⁷ G. B. Arnold, Phys. Rev. B **18**, 1076 (1978).
- ⁴⁸ A. L. Gudkov, M. Y. Kupriyanov, and K. K. Likharev, Zh. Eksp. Teor. Fiz. **94**, 319 (1988) [Sov. Phys. JETP **67**, 1478 (1988)].
- ⁴⁹ The matrix Green's functions for both superconductors and normal-metal interlayer can be expressed through the reflection amplitudes a_1 , a_2 , b_1 , and b_2 , see Refs.^{40,46}.
- ⁵⁰ G. Blatter, V. B. Geshkenbein, and L. B. Ioffe, Phys. Rev. B **63**, 174511 (2001); L. B. Ioffe, V. B. Geshkenbein, M. V. Feigelman, A. L. Fauchere, and G. Blatter, Nature (London) **398**, 679 (1999).

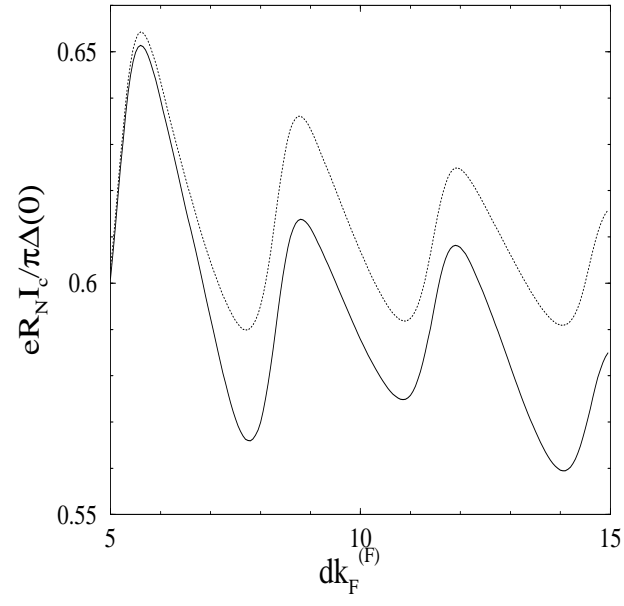


FIG. 1: Maximum current I_c as a function of d for $T/T_c = 0.1$, $\kappa = 1$, $Z = 1$, and for $h/E_F^{(F)} = 0.01$ (solid curve), and for $h = 0$ (dotted curve). In all illustrations the superconductors are characterized by $\Delta/E_F^{(S)} = 10^{-3}$.

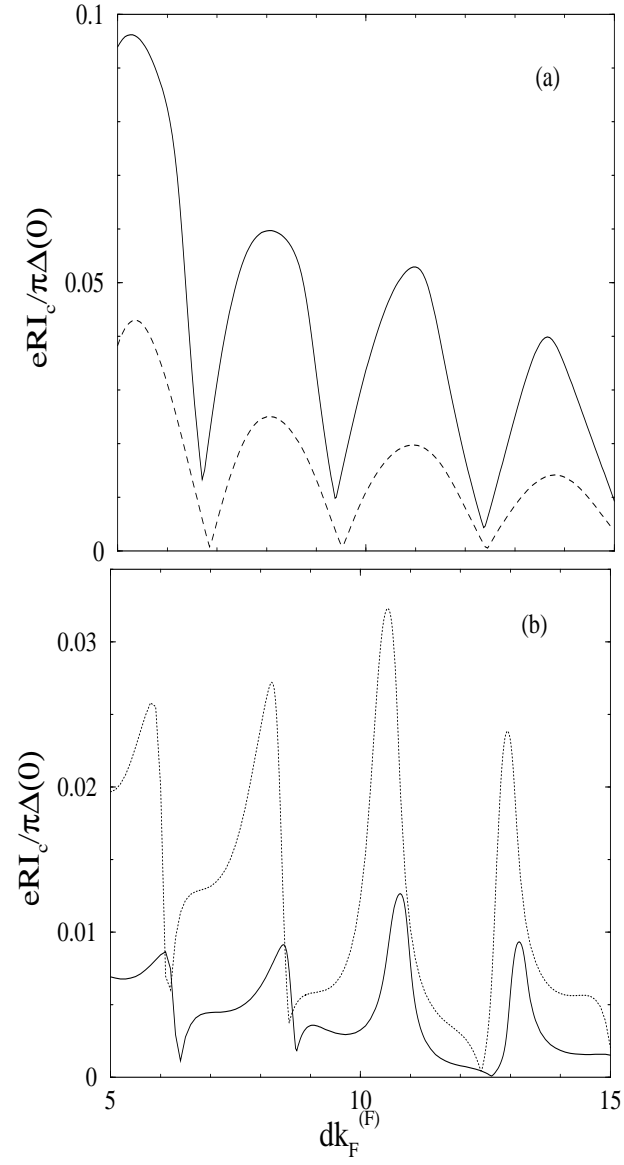


FIG. 2: Maximum current I_c as a function of d for $\hbar/E_F^{(F)} = 0.9$: (a) $Z = 0$, $\kappa = 1$, $T/T_c = 0.1$ (solid curve) and $T/T_c = 0.7$ (dashed curve); (b) $T/T_c = 0.1$, and $Z = 1$, $\kappa = 0.7$ (solid curve), $Z = 1$, $\kappa = 1$ (dotted curve). Dips in $I_c(d)$ separate alternating 0 and π states, starting with 0 state from the left.

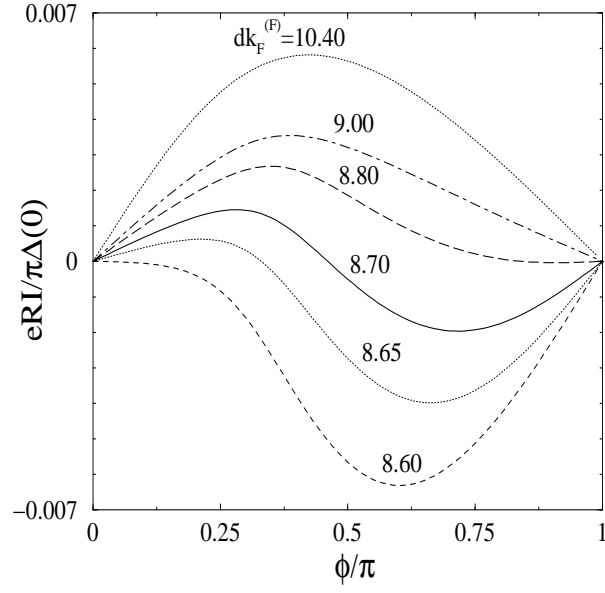


FIG. 3: Current-phase relation, $I(\phi)$, for $T/T_c = 0.1$, $h/E_F^{(F)} = 0.9$, $Z = 1$, $\kappa = 0.7$, and for five values of $dk_F^{(F)}$ in the vicinity of the crossover between 0 and π states ($d_c k_F^{(F)} = 8.72$), see solid curve in Fig. 2(b).

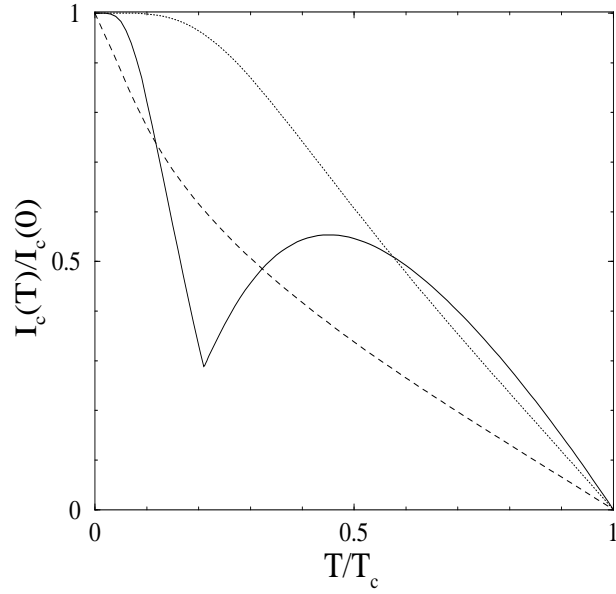


FIG. 4: Temperature variation of $I_c(T)$, normalized by $I_c(0)$, for $h/E_F^{(F)} = 0.92$, $Z = 1.2$, $\kappa = 1$, and for three values of $dk_F^{(F)} = 17$ (dotted curve), 17.23 (solid curve) and 17.4 (dashed curve).

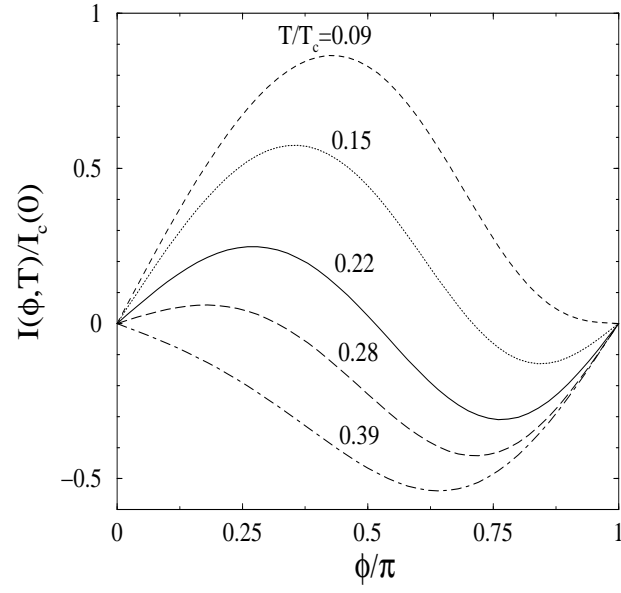


FIG. 5: Temperature variation of $I(\phi, T)$, normalized by $I_c(0)$, for $\hbar/E_F^{(F)} = 0.92$, $Z = 1.2$, $\kappa = 1$, $dk_F^{(F)} = 17.23$ and for five values of T/T_c in the vicinity of the transition from 0 to π state, see solid curve in Fig. 4.

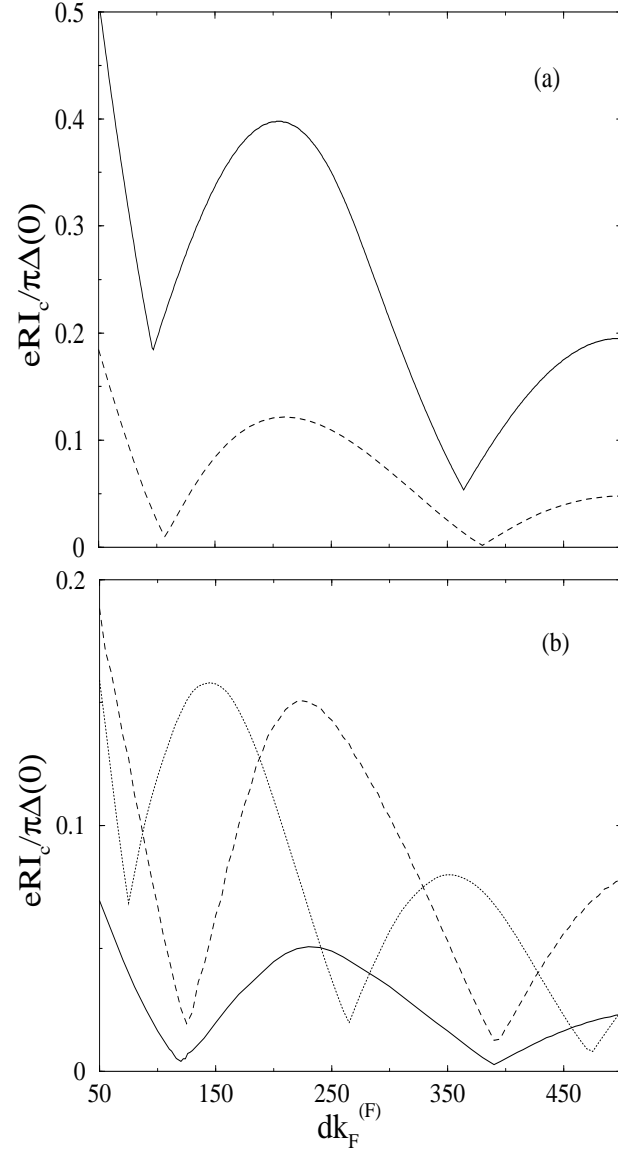


FIG. 6: Maximum current I_c as a function of d for $\hbar/E_F^{(F)} = 0.01$: (a) $Z = 0$, $\kappa = 1$, $T/T_c = 0.1$ (solid curve) and $T/T_c = 0.7$ (dashed curve); (b) $T/T_c = 0.1$, and $Z = 1$, $\kappa = 0.7$ (solid curve), $Z = 1$, $\kappa = 1$ (dashed curve), $Z = 0$, $\kappa = 0.7$ (dotted curve). Dips in $I_c(d)$ separate alternating 0 and π states, starting with 0 state from the left.